frontiers in Earth Science

ORIGINAL RESEARCH
published: 17 November 2021
doi: 10.3389/feart.2021.780343

Two-phased Mass Rarity and Extinction in Land Plants During the End-Triassic Climate Crisis

Sofie Lindström *

GEUS—Geological Survey of Denmark and Greenland, Copenhagen, Denmark

Greenhouse gas emissions from large-scale volcanism in the Central Atlantic Magmatic Province is considered to have caused the end-Triassic mass extinction (201.5 million years ago), but the impact on land plants has been debated. Here, abundance changes in spores and pollen record the devastating effects this volcanic induced climate crisis had on coastal and near-coastal lowland mire vegetation around the European epicontinental sea and the European Tethys margin. Combined stress from rising air temperatures and changing climate at the onset of the crisis was exacerbated by a rapidly rising sea-level resulting in fragmentation and destruction of coastal and near-coastal lowland mire habitats, causing mass rarity and extinctions primarily in gymnosperm trees and shrubs adapted to these environments. The devastation of these habitats was further amplified by a subsequent sea-level fall leaving pioneering opportunists and herbaceous survivors to colonize disturbed areas in an environment stressed by increased wildfire activity and enhanced soil erosion. The pioneering flora was severely decimated in a second mass rarity phase and ultimately extirpated. The second mass rarity phase occurred just prior to and at the onset of a prominent negative excursion in $\delta^{13}C_{org}$. A subsequent sea-level rise appears to have restored some of the near-coastal mire habitats allowing some of the plants to recover. The supraregional mass rarity during the end-Triassic crisis affected both previously dominant as well as rare plants and this resonates with ongoing and future climate change and attests to the vulnerability of coastal and lowland vegetation, especially rare plant species, to climatic and environmental disturbances, where rising sea-level threatens entire ecosystems.

Keywords: palynology, palaeoclimate, global warming, sea-level, mass extinction, Triassic—Jurassic boundary, spores, pollen

OPEN ACCESS

Edited by:
Jacopo Dal Corso, China University of Geosciences, China

Reviewed by:
Evelyn Kustatscher, Museum of Nature South Tyrol, Italy
Annette Götz, State Authority for Mining, Energy and Geology, Germany

***Correspondence:**
Sofie Lindström
sli@geus.dk

Specialty section:
This article was submitted to Paleontology, a section of the journal Frontiers in Earth Science

Received: *20 September 2021*
Accepted: *27 October 2021*
Published: *17 November 2021*

Citation:
Lindström S (2021) Two-phased Mass Rarity and Extinction in Land Plants During the End-Triassic Climate Crisis. Front. Earth Sci. 9:780343. doi: 10.3389/feart.2021.780343

1 INTRODUCTION

The end-Triassic mass extinction is generally recognized as one of the five major mass extinctions of the Phanerozoic (Sepkoski, 1996; McGhee et al., 2013), but the severity of the crisis on the vegetation is still debated. Amongst the land plants only seed ferns of the family Peltaspermaceae became extinct during the end-Triassic crisis (McElwain and Punyasena, 2007). However, on lower taxonomic levels extinctions are estimated to be higher, with up to 95% of species locally (McElwain et al., 1999). Estimating the severity of the crisis in land plants is complicated by provinciality and conflicting records between extinctions based on fossil leaf taxa and those based on spores and pollen (Bond and Wignall, 2014; Lindström, 2016; Barbacka et al., 2017). However, extinctions in spore and pollen taxa

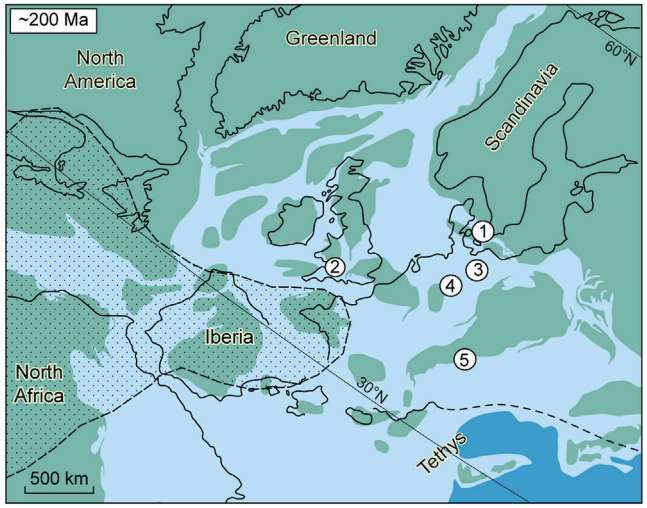

FIGURE 1 | Palaeogeographic map (after Blakey, 2014) of the European epicontinental sea and the northern Tethys margin, showing the location of the studied cored wells Stenlille-1 and -4, and other localities compared with in the text.

vary globally between 17 and 73% and for most of the taxa that went extinct, the parent plant affinity is not fully resolved or even unknown (Lindström, 2016). Likely, many of the spore-producing plants that disappeared at the end of the Rhaetian or in the earliest Hettangian were plants with ecological preferences that resulted in low preservation potential for their macroscopic remains, e.g. epiphytic plants or plants growing in sites with little potential for fast burial. From an ecological perspective, the crisis amongst land plants at the end of the Triassic was profound, with replacement or major disruptions of the terrestrial ecosystems (McGhee et al., 2013; Lindström, 2016). Recently, mass rarity, i.e. the reduction in the numerical abundances and/or the reduction in geographic ranges of several species, was suggested as a more robust measure of the severity of a biotic crisis than taxonomic extinction (Hull et al., 2015). In plant ecology and ecosystem analysis, rarity is a key factor when establishing whether a taxon is at risk of becoming endangered or extinct (Stohlgren and Kumar, 2013), but it is not often discussed for the big five biotic crises.

Here, two high resolution palynological records of the Danish Basin are used to assess whether mass rarity amongst land plants played a role in the end-Triassic crisis scenario. The marine TJB succession of the cored Stenlille-1 and -4 wells on Sjælland, Denmark (**Figure 1**), are well constrained by palynology, $\delta^{13}C_{org}$-isotopes and other geochemical proxies, and can be correlated primarily with other NW European TJB strata, but also globally (Lindström et al., 2017b). Deposition took place in a shoreface to offshore setting in the northwestern part of an epicontinental sea that covered large parts of Europe. The two wells are situated 3.5 km apart on opposite sides of a gentle salt dome and exhibit minor variations in the sedimentary record. Two negative excursions in $\delta^{13}C_{org}$, the Marshi CIE and the Spelae CIE, can be correlated with TJB sections in the Tethys and Panthallassic oceans, where the last occurrence of typical Triassic and the first occurrence of typical Jurassic ammonoids bracket the marine mass extinction interval (Lindström et al., 2017b, 2021). Both these excursions have been interpreted to reflect massive volcanic degassing of ^{12}C to the atmosphere from the CAMP, which could have acted as a trigger for the extinction (Hesselbo et al., 2002; Ruhl and Kürschner, 2011). In addition, Hg-anomalies in the succession provide a link to other Hg-records across the TJB and to the CAMP volcanism (Lindström et al., 2019; Lindström et al., 2021).

2 RESULTS

2.1 From Terrestrial Ecosystem Stability to Mass Rarity

The palynological records show that terrestrial vegetation of the extensive coastal areas and lowlands of the Danish Basin was remarkably stable during the middle Rhaetian (**Figure 2**). Variations in climate and sea level likely influenced vegetation changes on land as well as changes in depositional environment (Nielsen, 2003), contributing to abundance variations in the palynological records of the Gassum Formation (**Figure 2**). The pollen records show that cheirolepidiacean and taxodiacean/cupressacean conifers dominated the vegetation (**Figure 2**), occupying the upper canopy tier in drier and wetter environments, respectively (**Tables 1** and **2**; **Figure 3A**). Apart from these and *Ricciisporites tuberculatus*, most other typical Rhaetian tree pollen taxa were less common, but their parent plants were still important contributors to the upper canopy. The Rhaetian mire forests were most likely multi-storeyed and lush, with mid-canopy elements including very rare Erdtmannithecales, rare Bennettitales and Ginkgoales/Cycadales, and common Caytoniales (**Tables 1** and **2**; **Figure 3A**), similar in composition to macroplant assemblages described from Greenland, southern Sweden and Germany (McElwain et al., 2007; Pott and McLoughlin, 2011; Van Konijnenburg-Van Cittert et al., 2018). Understorey plants, including ferns, lycophytes, bryophytes and sphenophytes, were generally rare to common and many of these plants were probably adapted to living in the shade of the trees or even as epiphytes on the trees (**Figure 3A**).

Two phases of mass rarity are evident in the Stenlille pollen records, here referred to as MR1 and MR2, respectively (**Figure 2**). MR1 occurs within the lowermost part of the Fjerritslev Formation (**Figure 2**) and encompasses the upper part of a black shale and the lowermost part of the succeeding "grey siltstone" interval of the Fjerritslev Formation (Lindström et al., 2017b) (**Figure 2**). At MR1, upper canopy plants appear to have been particularly hard hit. Both the coastal, salinity tolerant and xerophytic cheirolepidiacean conifers, as well as the taxodiacean/cupressacean conifers that preferred wet habitats like mires and estuaries (Mussard et al., 1997), were severely

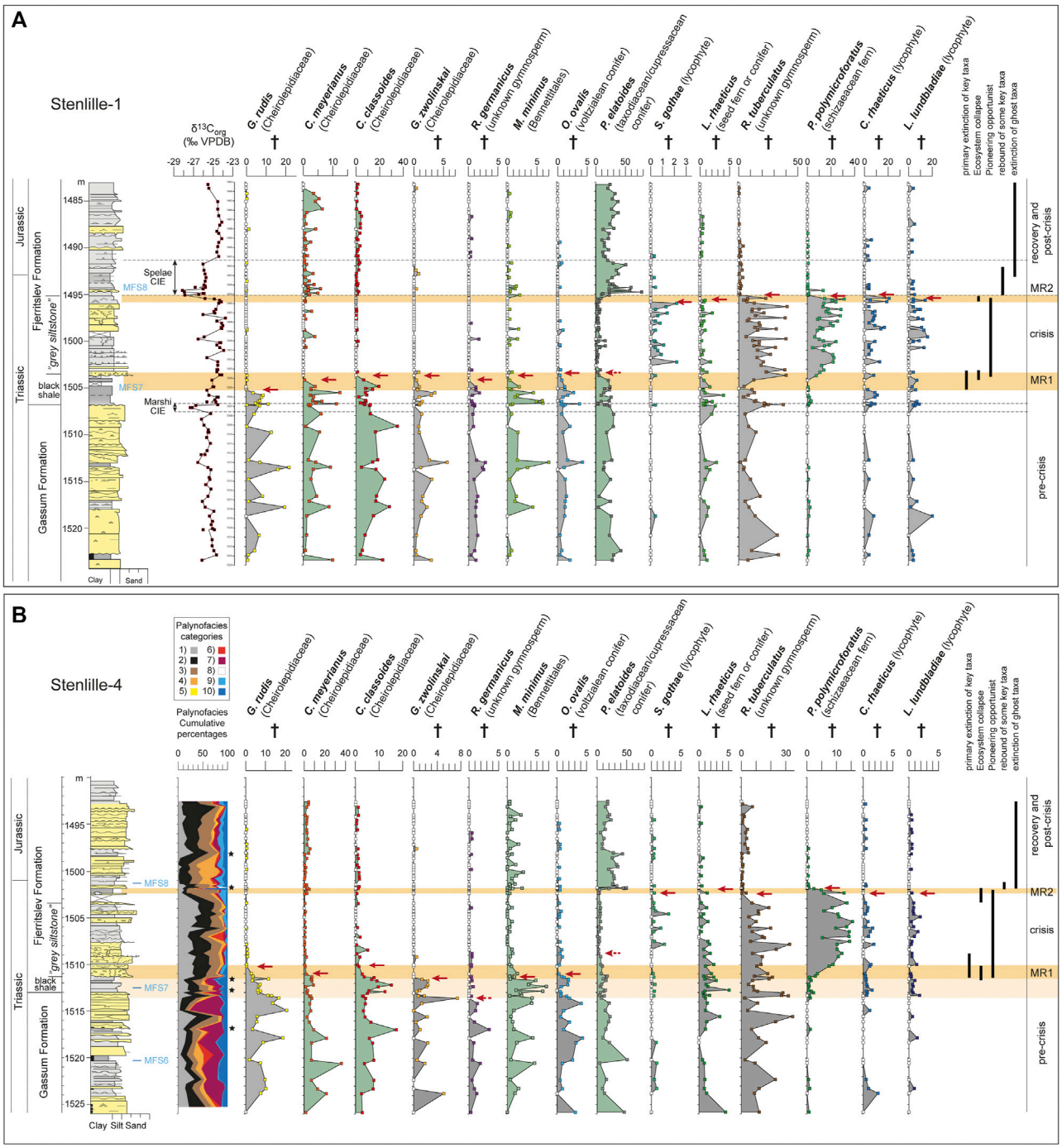

FIGURE 2 | Abundances of selected representative spore-pollen taxa in the Triassic–Jurassic boundary successions of the **(A)** Stenlille-1 and **(B)** Stenlille-4 cored wells. **(A)** also displays the $\delta^{13}C_{org}$ record of Stenlille-1, the position of the Marshi and Spelae CIEs, and of the maximum flooding surfaces (Nielsen, 2003, Lindström et al., 2021). **(B)** also shows the cumulative percentages of palynofacies categories: 1) black opaque clasts, 2) black wood remains, 3) brown wood remains, 4) plant tissue, 5) cuticles, 6) Amorphous organic matter, 7) marine phytoplankton, 8) freshwater microalgae, 9) spores, 10) pollen. The spore-pollen counts for Stenlille-1 and -4 are listed in **Supplementary Tables S1, S2**, respectively. Black stars mark observations of char.

reduced in abundances within a c. 2 m thick interval from the middle of the black shale in the Stenlille-1 record (**Figure 2A**; **Table 1**). Four different cheirolepidiacean pollen species exhibit rarity at this level commencing with *Granuloperculatipollis rudis*, followed in ascending order by *Classopollis meyerianus*, *Geopollis zwolinskai* and *C. classoides* (**Figure 2**). Rarity is also registered in *Rhaetipollis germanicus, Monosulcites minimus, Ovalipollis ovalis* and *Perinopollenites elatoides,* showing that other tree taxa were

TABLE 1 | Botanical affinity, habit, leaf morphology, pollination strategy, and environmental preferences for the parent plants affected at MR1 and MR2.

Spore or pollen taxon	Mother plant Order Family	Habit	Leaf morphology	Pollen dispersal	Ecological preference	MR1	MR2
Classopollis classoides	Conifer Coniferales Cheirolepidiaceae	Upper canopy	Scaly leaf shoots	Wind	Xerophytic, salinity tolerant	Non-permanent rarity	Recovery
Classopollis meyerianus	Conifer Coniferales Cheirolepidiaceae	Upper canopy	Scaly leaf shoots	Wind	Xerophytic, salinity tolerant	Non-permanent rarity	Recovery
Granuloperculatipollis rudis	Conifer Coniferales Cheirolepidiaceae	Upper canopy	Scaly leaf shoots	Wind	Xerophytic, salinity tolerant	Permanent rarity	Extirpation
Geopollis zwolinskai	Conifer Coniferales Cheirolepidiaceae	Upper canopy	Scaly leaf shoots	Wind	Xerophytic, salinity tolerant	Permanent rarity + Extirpation	—
Rhaetipollis germanicus	Gymnosperm Unknown	Unknown, here placed in mid-canopy	Unknown	Unknown	Unknown	Permanent rarity + Extirpation	—
Perinopollenites elatoides	Conifer Coniferales Taxodiaceae/ Cupressaceae	Upper canopy	Needle-like leaves	Wind	Moisture loving, mire	Non-permanent rarity	Recovery
Ovalipollis ovalis	Conifer Voltziales Unknown	Upper canopy	Needle-like leaves	Wind	Xerophytic	Permanent rarity	Extirpation
Monosulcites minimus	Seed fern Bennettitales Unknown	Mid canopy	Segmented or entire-margined	Insect	Deltaic and disturbed environments, mire	Non-permanent rarity	Recovery
Lunatisporites rhaeticus	Seed fern or Conifer Voltziales Unknown	Upper canopy	?Needle-like leaves	Wind	?Xerophytic	Permanent rarity	Permanent rarity + Extirpation
Semiretisporis gothae	Lycophyte	Ground cover	—	Water	Lowlands, hygrophytic	—	Permanent rarity + Extirpation
Cingulizonates rhaeticus	Lycophyte	Ground cover	—	Water	Lowlands, hygrophytic	—	Permanent rarity + Extirpation
Limbosporites lundbladiae	Lycophyte	Ground cover	—	Water	Lowlands, hygrophytic	—	Permanent rarity + Extirpation
Polypodiisporites polymicroforatus	Fern Filicales Schizaeaceae	Ground cover	—	Water	Disturbed environments, ? hygrophytic	—	Permanent rarity + Extirpation
Ricciisporites tuberculatus	Gymnosperm	Unknown, here placed in mid-canopy	Unknown	Insect? Animal?	Unknown	—	Permanent rarity + Extirpation

also affected (**Figure 2A**). The affinity of *R. germanicus* is unknown, but *O. ovalis* may have been produced by voltzialean conifers (Scheuring, 1970), and *M. minimus* by a bennettitalean parent plant (Pott et al., 2016). The Cheirolepidiacean, taxodiacean/cupressacean and voltzialean conifers had scale- or needle-like leaves that would make them more fire prone than e.g., bennettitaleans that had elongated entire-margined or segmented leaves (Belcher et al., 2010) (**Table 1**). Wildfires under high temperatures indicative of crown fires in fire-prone vegetation are known to have occurred in the mid-Rhaetian mires (Petersen and Lindström, 2012). Palynofacies analyses of the Stenlille-4 samples show some intervals in the Gassum Formation where increased amounts of black phytoclasts and wood remains indicate that more intense wildfires may have occurred at times (**Figure 2B**). Rhaetian bennettitaleans seem to have had an ecological preference for highly disturbed and deltaic habitats (Pott, 2014), and *M. minimus* was found to be common to abundant in the fire struck Rhaetian mires of the Danish Basin (Petersen and Lindström, 2012). Except for the Bennettitales that may have been insect pollinated (Pott, 2014), the tree taxa affected at MR1 are all considered to have been wind pollinated (**Table 1**). In the Stenlille-4 record MR1 appears to be extended from the uppermost part of the Gassum Formation to lower part of the "grey siltstone" interval (**Figure 2B**). Discrepancies between the upper part of MR1 in this record and Stenlille-1 likely relates to the fact that the base of the "grey siltstone" in Stenlille-4 contains clay clasts probably derived from the black shale (**Figure 2**). Apart from the probable reworking of black shale material into the lowermost "grey siltstone", the overall pattern is similar in the two wells. Although neither the parent plants of *Classopollis classoides, C. meyerianus, Perinopollenites elatoides* nor

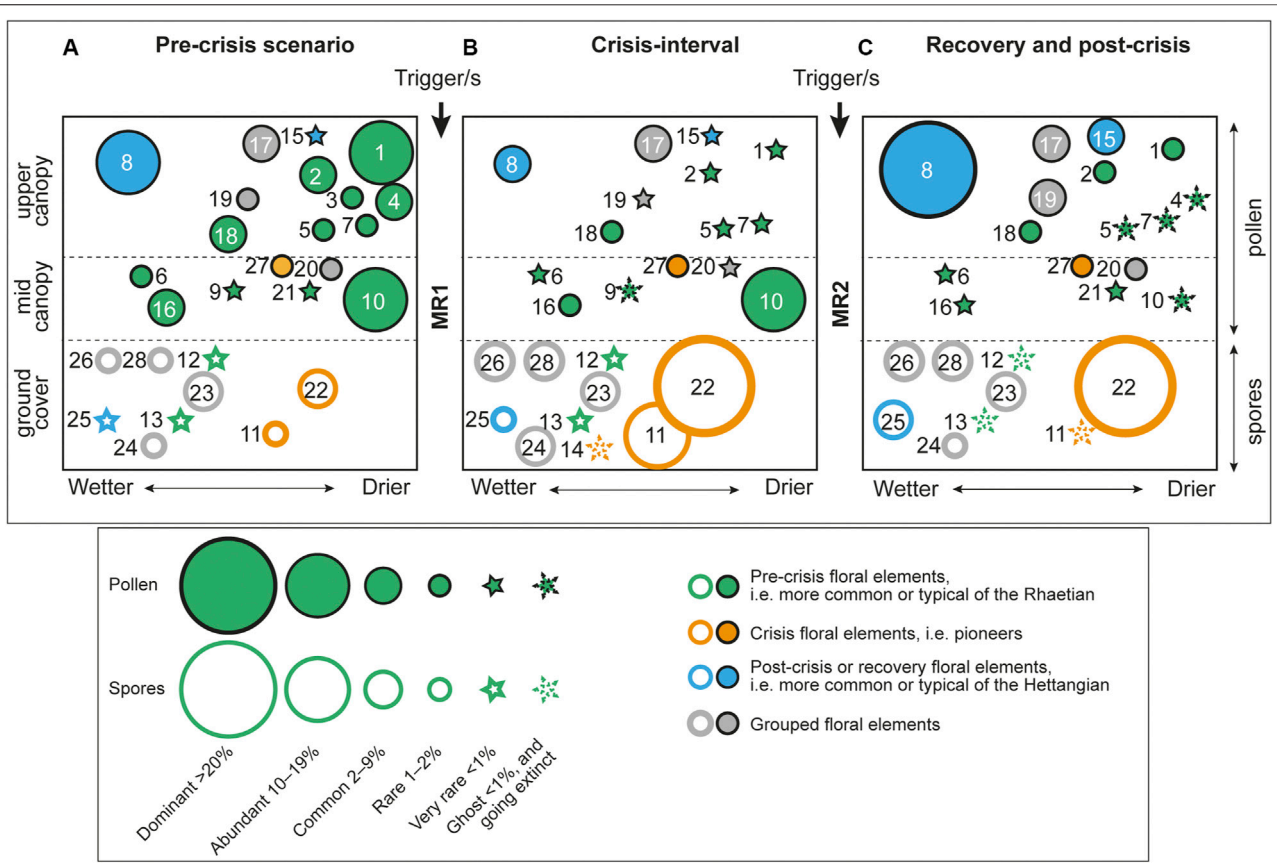

FIGURE 3 | Schematic bubble diagrams illustrating vegetation composition in the Danish Basin during **(A)** the pre-MR1 interval, **(B)** the floral crisis interval, **(C)** the post-MR2 and recovery interval, based on mean relative spore-pollen abundances in Stenlille-1. Numbers in the diagrams refer to twenty-eight specific spore-pollen taxa, namely: 1. *Classopollis classoides*, 2. *Classopollis meyerianus*, 3. *Geopollis zwolinskai*, 4. *Granuloperculatipollis rudis* (all cheirolepidiacean conifers), 5. *Lunatisporites rhaeticus* (seed fern of conifer); 6. *Monosulcites minimus* (Bennettitales); 7. *Ovalipollis ovalis* (voltzialean conifer); 8. *Perinopollenites elatoides* (taxodiacean/cupressacean conifer); 9. *Rhaetipollis germanicus* (unknown affinity); 10. *Ricciisporites tuberculatus* (unknown gymnosperm); 11. *Polypodiisporites polymicroforatus* (schizaeacean fern); 12. *Cingulizonates rhaeticus* (unknown lycophyte); 13. *Limbosporites lundbladiae* (unknown lycophyte); 14. *Semiretisporis gothae* (unknown lycophyte); 15. *Pinuspollenites minimus* (pinacean conifer); 16. *Vitreisporites pallidus* and *V. bjuvensis* (both Caytoniales); 17. Bisaccates (other than specified), 18. *Alisporites* spp. (seed ferns), 19. Non-saccate conifers (other than specified), 20. Monosulcate non-conifer pollen (other than specified), 21. *Eucommiidites* spp. (Erdtmannithecales), 22. *Deltoidospora* spp. (dipterid and matoniacean ferns), 23. Fern spores (other than specified), 24. Lycophytes (other than specified), 25. *Calamospora* spp. (Equisetales), 26. Bryophytes, 27. *Chasmatosporites* spp. (Ginkgo or Cycads), and 28. *Osmundacidites/Baculatisporites/Punctatisporites* spp. (osmundacean ferns). Mean abundance values can be found in **Table 2**.

Monosulcites minimus were extirpated in the end-Triassic extinction, the cheirolepidiacean conifers that produced *G. zwolinkai* and *G. rudis*, as well as the voltzialean conifer that shed *O. ovalis* and the unknown parent plant of *R. germanicus*, were all victims of the crisis.

2.2 Ecological Upheaval and Pioneering Plants

The ecological disruption during MR1 resulted in a major reduction of the upper and mid-canopy tree elements, suggesting major deforestation in the area and a marked shift towards a more open landscape (**Tables 1** and **2**; **Figure 3B**). Marked and consistently increased levels of black phytoclasts and black wood remains, and significantly decreased amounts of spores and pollen compared to prior to MR1 may indicate that increased wildfire (**Figure 2B**). Both the vegetation density and volume were likely severely decreased during this floral crisis interval as indicated by low TOC values (Lindström et al., 2019), and by significantly lower amounts of spores and pollen during this interval (**Figure 2B**). The deforestation allowed some previously less prominent taxa to flourish during the deposition of the "grey siltstone" (**Figures 1**, **2**). In particular the understorey spore-producing schizaeacean (*Polypodiisporites polymicroforatus* spores) and dipterid and/or matoniaceous ferns (Van Konijnenburg-Van Cittert et al., 2020) (*Deltoidospora* spores; not shown on **Figure 2**) seem to have benefitted from the open landscape (**Table 2**; **Figure 3B**). These opportunistic ferns had a significantly faster life cycle than trees and could perhaps reproduce both sexually and through asexual spreading via rhizomes. These ferns flourished together with an unknown, possibly ruderal, gymnosperm (*Ricciisporites*

tuberculatus pollen) (Kürschner et al., 2014) that also increased in abundance compared to in the Gassum Formation. A similar vegetation response has been documented across Europe and interpreted as reflecting widespread distribution of pioneering plant communities after deforestation (van de Schootbrugge et al., 2009; Lindström, 2016; Lindström et al., 2017b; Gravendyck et al., 2020). Interestingly, *Monosulcites minimus* is significantly decreased during the deforestation interval, i.e. the "grey siltstone" beds, despite the parent plants possible preference to disturbed habitats (Pott, 2014) (**Figure 2**). Some typical Rhaetian spore-pollen taxa, e.g., the lycophyte spores *Limbosporites lundbladiae* and *Cingulizonates rhaeticus*, and the probable conifer or seed fern pollen *Lunatisporites rhaeticus*, show none or only marginal changes in abundance during this interval (**Figure 2**). Another typical Rhaetian lycophyte spore, *Semiretisporis gothae*, even increased in abundance during the deposition of the "grey siltstone" beds.

2.3 Mass Rarity and Recovery

In the uppermost part of the "grey siltstone" beds, a second mass rarity event, MR2, was instigated with the virtual disappearance of the low-abundance species *S. gothae*, *L. rhaeticus, C. rhaeticus,* and *L. lundbladiae* (**Figures 2**, **3C**). Two of the opportunistic palynofloral elements in the "grey siltstone" beds, *P. polymicroforatus* and *R. tuberculatus,* also show marked abundance losses, reflecting that the collapse of the pioneering ecosystem occurred during MR2 (**Figure 2**). MR2 coincided with the onset and first negative peak of the Spelae CIE (**Figure 2**), which coincides with a sudden relative increase in the equisetalean spore *Calamospora tener* and in the freshwater algae *Botryococcus braunii* (CCM zone in (Lindström et al., 2017b). As equisetaleans preferred wet environments like riverbanks or lake shores, this signals an increase in freshwater input at that time. After this there was a return of, in particular, the taxodiacean/cupressacean (*P. elatoides* pollen), but also to a lesser extent cheirolepidiacean (*C. meyerianus* and *C. classoides* pollen) and bennettitalean (*M. minimus* pollen) trees (**Figure 2**). Although cupressacean conifers appear to have returned in large numbers signalling re-establishment of coastal mires, the drier coastal habitats that supported the cheirolepidiacean conifers appear to have been greatly diminished (**Tables 1** and **2**; **Figure 3C**). In general, the post-crisis vegetation appears less dense in the upper canopy while the mid-canopy tier seems almost eradicated, similar to macroplant fossil observations in East Greenland (McElwain et al., 2007). The post-crisis vegetation contained several rare or ghost taxa, the latter including e.g., *G. rudis, O. ovalis, L. rhaeticus, P. polymicroforatus* and *R. tuberculatus,* that were victims of the crisis (**Figure 3C**). Later, *Pinuspollenites minimus,* a previously rare pinacean conifer pollen increased in abundance during the post-crisis and recovery interval, probably inhabiting hinterland or drier areas (Lindström, 2016) (**Figure 3C**).

2.4 Diversity Patterns Reveal Onset of Disturbances

Diversity indices provide additional clues to the timing and severity of the environmental changes that led to the mass rarity phases. In accordance with the intermediate disturbance hypothesis (IDH) (Svensson et al., 2012), two intervals where species richness increased and peaked indicate that the ecosystem was subjected to disturbances of intermediate magnitude and/or frequency; namely intermediate disturbance 1 (ID1) and 2 (ID2) (**Figure 4**). At ID1 species richness increased and peaked just prior to and during the lower part of MR1 (**Figure 4**), indicating an intermediate level of disturbance that hindered competitive exclusion by supressing species that were previously dominant and allowing new species to colonize free space (Svensson et al., 2012). This is reflected by the initial increase in richness coinciding with a minimum in dominance, <0.1, and an increase in evenness to >0.8 (**Figure 4**). Just prior to MR1, while species richness was still high, evenness dropped continuously to the top of MR1 (**Figure 4**), indicating high level disturbances promoting dominance of a few disturbance specialists, namely *P. polymicroforatus*, *R. tuberculatus* and *Deltoidospora* spp. (**Figure 2**). The decline in evenness continued to the top of MR1 as species richness also declines, reflecting a subsequent loss in biodiversity (**Figure 4**).

At ID2 in the upper part of the "grey siltstone" beds, richness again reached maximum levels indicating intermediate disturbance (**Figure 4**). At the top of the beds, richness fell successively and reached a minimum during MR2 (**Figure 4**). This coincided with a fall in dominance and a rise in evenness, suggesting that the taxa that were ecologically dominant during the "grey siltstone" beds were now suffering, whereas other species were recovering or establishing. The diversity indices suggest that conditions improved after the Spelae CIE and the palynology suggests that some of the previously lost coastal habitats were restored, as primarily taxodiacean/cupressacean, but also to lesser extent cheirolepidiacean, conifers increase in abundance (**Figures 1**–**3**).

3 DISCUSSION

3.1 Comparison With Other Records

3.1.1 St. Audrie's Bay, United Kingdom

The St. Audrie's Bay succession (**Figures 1**, **5**) is one of the extensively studied key localities for the TJB, and it is well constrained by palynology, ammonoids and organic C-isotopes (Hesselbo et al., 2002; Hesselbo et al., 2004). Hesselbo et al. (2004) indicated that a maximum flooding surface (MFS) is present in the middle of the Westbury formation, around the level of the Marshi CIE, but they could not specify the exact location. Maximum abundances of dinoflagellate cysts (Bonis et al., 2010) indicate that the MFS could be located higher, in the uppermost part of the Westbury Formation and lower to upper Cotham Member of the Lilstock Formation. It is within this interval that several spore-pollen taxa begin to decline markedly in abundance. *Granuloperculatipollis rudis* is the first taxon to exhibit rarity already in the uppermost Westbury Formation. Then *Perinopollenites* elatoides, which was never common, declines in abundance and *Ovalipollis ovalis* becomes rare in the uppermost lower Cotham Member and at this level *Classopollis meyerianus* also shows a marked decline in abundance, although it never becomes rare (Bonis et al., 2010,

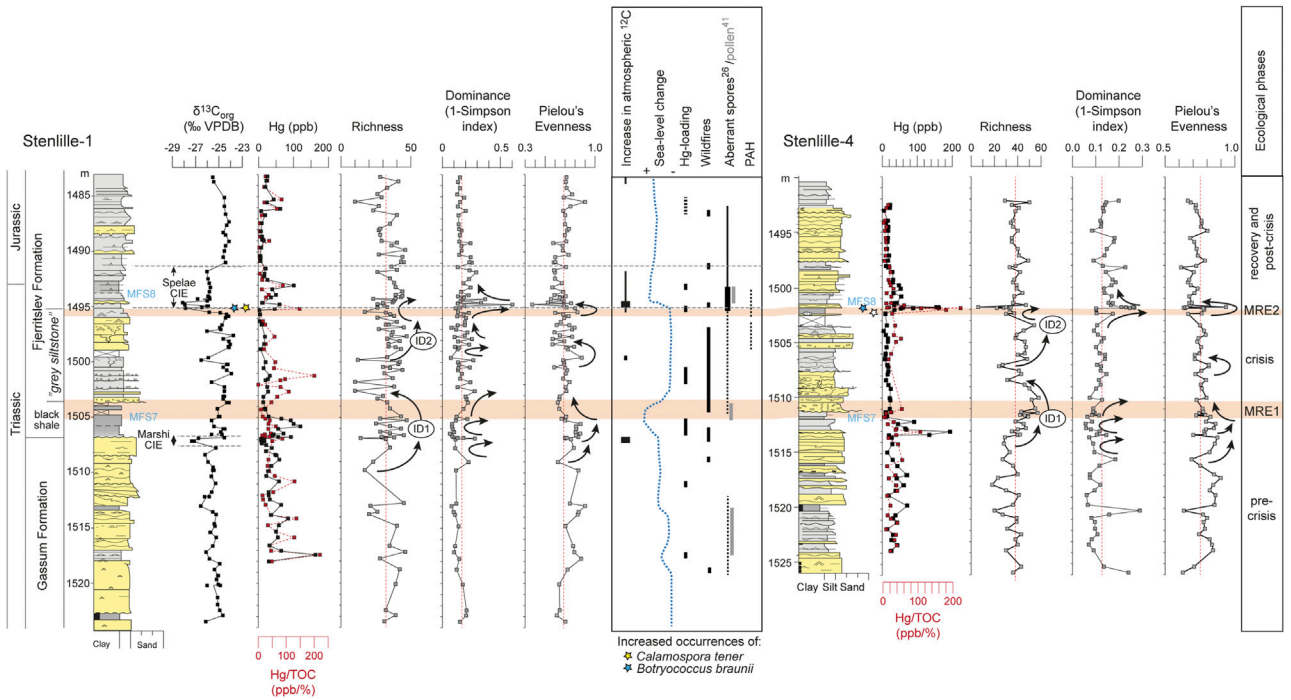

FIGURE 4 | Comparison of species richness, dominance (1-Simpson index), and Pielou's evenness in Stenlille-1 and Stenlille-4. ID1 and ID 2 refer to two intervals with increased to maximum values in species richness indicate intermediate disturbance (Connell, 1978; Svensson et al., 2012). Hg and Hg/TOC records have been interpreted to reflect volcanic pulses of the CAMP (Lindström et al., 2021). Thin stippled red lines indicate mean level of the respective diversity indices.

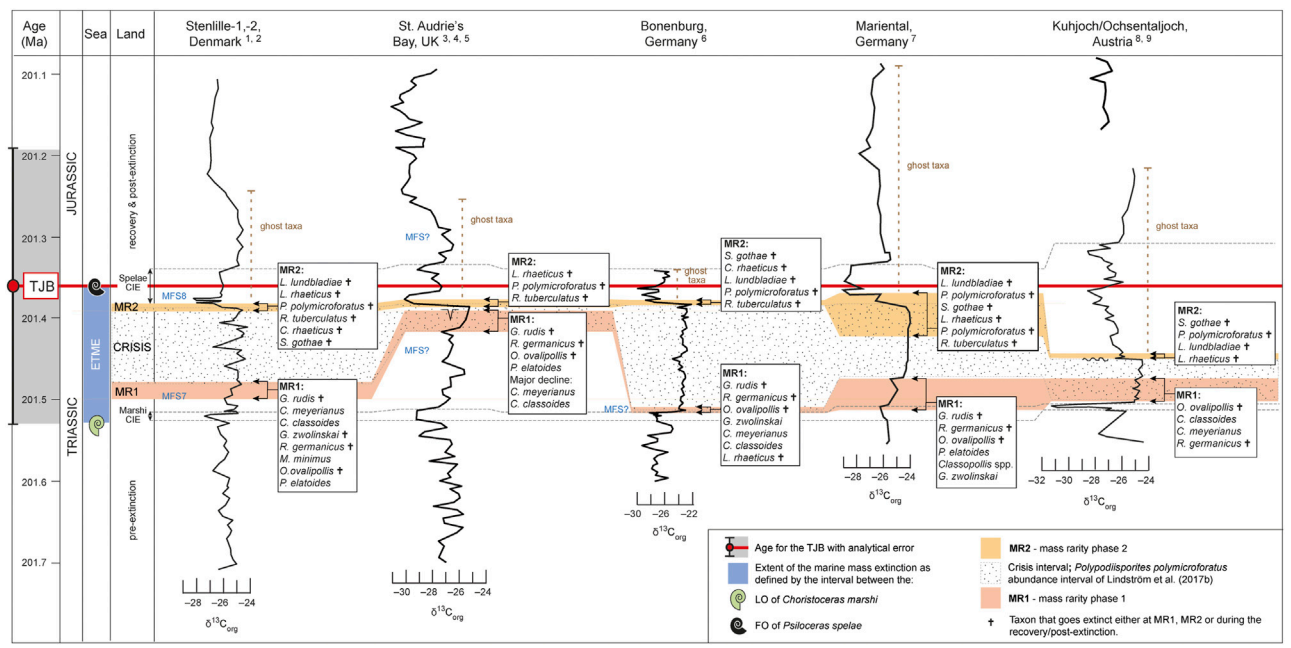

FIGURE 5 | Correlation of $\delta^{13}C_{org}$-records, mass rarity phases (MR1 and 2) and crisis interval [i.e. *Polypodiisporites polymicroforatus* abundance interval of Lindström et al. (2017b)] in Stenlille-1, St. Audrie's Bay, Bonenburg, Mariental and Kuhjoch. The recorded taxa are also shown in **Table 3**. Numbers after the localities refer to the following references: 1. Lindström et al. (2017b), 2. Lindström et al. (2021), 3. Hesselbo et al. (2002), 4. Hesselbo et al. (2004), 5. Bonis et al. (2010), 6. Gravendyck et al. (2020); Heunisch et al. (2010), 8. Bonis et al. (2009), 9. Hillebrandt et al. (2013). The correlation is based on Lindström et al. (2017b), Lindström et al. (2021).

TABLE 2 | Mean percentage data for the various spore-pollen taxa or groups of taxa shown in **Figure 3** as well as assumed forest level and climate preference.

Nr. on Figure 3	—	Taxon or group of taxa	Pre-extinction	Crisis	Recovery and post-extinction	Forest level	Climate preference
1	Pollen	*Classopollis classoides*	12.4%	0.2%	1.3%	Upper canopy	Xerophytic
2	Pollen	*Classopollis meyerianus*	3.9%	0.3%	1.8%	Upper canopy	Xerophytic
3	Pollen	*Geopollis zwolinskai*	1.3%	0.0%	0.0%	Upper canopy	Xerophytic
4	Pollen	*Granuloperculatipollis rudis*	5.5%	0.0%	0.1%	Upper canopy	Xerophytic
5	Pollen	*Lunatisporites rhaeticus*	1.0%	0.3%	0.1%	Upper canopy	Xerophytic
6	Pollen	*Monosulcites minimus*	1.8%	0.2%	0.3%	Mid canopy	Wet
7	Pollen	*Ovalipollis ovalis*	1.2%	0.1%	0.1%	Upper canopy	Xerophytic
8	Pollen	*Perinopollenites elatoides*	18.8%	4.2%	27.4%	Upper canopy	Wet
9	Pollen	*Rhaetipollis germanicus*	0.9%	0.1%	0.0%	Unknown	Unknown
10	Pollen	*R. tuberculatus*	14.1%	16.9%	0.7%	Unknown	Xerophytic
11	Spores	*Polypodiisporites polymicroforatus*	1.0%	15.9%	0.6%	Ground cover	Drier
12	Spores	*Cingulizonates rhaeticus*	0.3%	0.6%	0.1%	Ground cover	Wet
13	Spores	*Limbosporites lundbladiae*	0.3%	0.4%	0.1%	Ground cover	Wet
14	Spores	*Semiretisporis gothae*	0.0%	0.4%	0.0%	Ground cover	Wet
15	Pollen	*Pinuspollenites minimus*	0.7%	0.4%	8.1%	Upper canopy	Xerophytic
16	Pollen	*Vitreisporites* spp.	3.3%	1.3%	0.9%	Mid canopy	Xerophytic
17	Pollen	Other bisaccates	8.0%	5.7%	2.9%	Upper canopy	Xerophytic
18	Pollen	*Alisporites* spp.	2.3%	1.8%	1.1%	Upper canopy	Xerophytic
19	Pollen	Other non-saccate conifers	1.7%	0.6%	2.0%	Upper canopy	Xerophytic
20	Pollen	*Monosulcites* spp. other	1.3%	0.7%	1.9%	Upper canopy	Unknown
21	Pollen	*Eucommiidites* spp.	0.4%	0.0%	0.1%	?Mid canopy	Drier
22	Spores	*Deltoidospora* spp.	8.7%	25.5%	23.8%	Ground cover	Drier
23	Spores	Other ferns (minus *Osmundaceae*)	3.9%	8.3%	7.2%	Ground cover	Wet
24	Spores	Other lycophytes	1.7%	2.2%	1.9%	Ground cover	Wet
25	Spores	*Calamospora* spp.	0.5%	1.9%	5.0%	Ground cover	Wet
26	Spores	Bryophytes total	1.8%	2.2%	4.9%	Ground cover	Wet
27	Pollen	*Chasmatosporites* spp.	1.2%	1.7%	1.2%	Upper canopy	Drier
28	Spores	*Osmundaceae* total	1.3%	3.9%	6.0%	Ground cover	Wet

Figures 3, **4** therein). *Rhaetipollis germanicus* becomes rare just at the level marked by desiccation cracks (see below) and this is also where *C. classoides* first drops markedly in abundance (Bonis et al., 2010) (**Figure 5**). The presence of an erosion surface with prominent desiccation cracks up to 90 cm deep at the top of the lower Cotham member indicates a hiatus at that level in the succession (Hesselbo et al., 2004) (**Figure 5**). Sedimentary structures including flat-topped ripples indicate water depth of just a few meters in the upper Cotham Member of the Lilstock Formation and thus the culmination of a regressive event (Hesselbo et al., 2004). This corresponds stratigraphically to the sea-level fall in the Danish and North German Basins. Thus, a first phase of mass rarity (MR1) can be recognized in the lower Cotham Member, below the desiccation cracks (**Table 3**; **Figure 5**). It is possible that most of the crisis interval at St. Audrie's Bay is missing Lindström et al. (2017b). In addition, several of the taxa reviewed herein where not listed in the palynological record from St. Audrie's Bay, namely *Cingulizonates rhaeticus*, *Limbosporites lundbladiae*, *Semiretisporis gothae*, and *Geopollis zwolinskai* (Bonis et al., 2010) (**Table 3**), so their responses cannot be assessed. A second mass rarity phase (MR2) can be distinguished within a narrow interval above the desiccation cracks, encompassing the onset of the Spelae CIE, with rarity in *Lunatisporites rhaeticus, Perinopollenites elatoides, Polypodiisporites polymicroforatus* and *Ricciisporites tuberculatus* (**Table 3**; **Figure 5**). The MR2 interval in St. Audrie's Bay corresponds more or less to the interval referred to as the "lower CIE" in by Fox et al. (2020), interpreted to represent a dramatic perturbation to the ecosystem by shallowing with increasing freshwater conditions and development of microbial mats. The onset of the Spelae CIE is in St. Audrie's Bay also associated with an increased abundance of the equisetalean spore *Calamospora tener*, which may suggest increased runoff from a nearby freshwater source where equisetalean plants may have thrived along riverbanks or lake shores.

3.1.2 Bonenburg, Germany

In the Bonenburg section (**Figures 1**, **5**), located in the German Basin, six taxa exhibit mass rarity during an interval stratigraphically equivalent with MR1, namely *Classopollis classoides, C. meyerianus, Geopollis zwolinskai, Granuloperculatipollis rudis, Ovalipollis ovalis* and *Rhaetipollis germanicus* (Gravendyck et al., 2020) (**Table 3**; **Figure 5**). The abundance drops in these taxa occur at or immediately after a peak in marine phytoplankton abundance, in particular the fully marine dinoflagellate cyst taxon *Rhaetogonyaulax rhaetica* in the upper part of the Contorta Beds, which suggests that this level represents a maximum transgression (Gravendyck et al., 2020). Only *G. rudis* disappears at this level. *Perinopollenites elatoides* is rare throughout the section and appears to have been unaffected. *Lunatisporites rhaeticus* is also rare but drops in abundance within the crisis interval (Triletes beds) (Gravendyck et al., 2020) (**Table 3**; **Figure 5**). At a level equivalent to MR2,

TABLE 3 | Comparison of mass rarities, extinctions and recoveries of the selected taxa on **Figure 1**, for Stenlille-1 and -4 (this paper), St. Audrie's Bay (United Kingdom; Bonis et al., 2010), Bonenburg (Germany; Gravendyck et al., 2020), Mariental (Germany; Heunisch et al., 2010), Kuhjoch (Austria; Bonis et al., 2009; Hillebrandt et al., 2013). The localities are correlated according to ref. 10[10]. In the case of Mariental, only *Classopollis* spp. is listed. Numbers for the seven lowest lines in the table refer to number of taxa affected during each phase.

	Stenlille-1				Stenlille-4				St. Audrie's bay				Bonenburg				Mariental				Kuhjoch			
Selected taxa	**MR1**	**Crisis**	**MR2**	**Post-crisis**	**MR1**	**Crisis**	**MR2**	**Post-crisis**	**MR1**	**Crisis**	**MR2**	**Post-crisis**	**MR1**	**Crisis**	**MR2**	**Post-crisis**	**MR1**	**Crisis**	**MR2**	**Post-crisis**	**MR1**	**Crisis**	**MR2**	**Post-crisis**
Classopollis classoides	x	—	—	R	x	—	—	R	(x)	—	—	R	x	—	R	—	x	—	R	—	—	(x)	R	—
Classopollis meyerianus	x	—	—	R	x	—	—	R	(x)	—	R	—	x	—	R	—	x	—	R	—	x	—	—	—
Geopollis zwolinskai	x	—	—	†	x, †	—	—	—	not listed				x	—	R	—	x	—	—	—	not listed			
Granuloperculatipollis rudis	x, †	—	—	—	x	†	—	—	x, †	—	—	—	x, †	—	—	—	†	—	—	—	x, †	—	—	—
Rhaetipollis germanicus	x, †	—	—	—	x	†	—	—	x	—	†	—	x	—	—	†	x, †	—	—	—	x, †	—	—	—
Monosulcites minimus	x	—	—	R	x	—	R	—	not listed				not specified				not listed				not listed			
Ovalipollis ovalis	x	—	—	†	x	—	—	†	x	—	†	—	x	—	—	†	x	—	—	†	x	—	—	†
Perinopollenites elatoides	x	—	R	—	—	X	R	—	x	—	—	R	not affected				x	—	R	—	not affected			—
Limbosporites lundbladiae	—	—	x	†	—	—	x	†	not listed				—	—	x	†	x	—	†	—	—	—	x	†
Lunatisporites rhaeticus	—	—	x	†	—	—	x	†	—	—	x, †		—	x		†	—	x	†	—	—	x, †	—	—
Polypodiisporites polymicroforatus	—	—	x	†	—	—	x	†	—	—	x	†	—	—	x, †	—	—	—	x	†	—	—	x	†
Ricciisporites tuberculatus	—	—	x	†	—	—	x	†	—	—	x	†	—	—	x	†	—	x	—	†	not affected			
Cingulizonates rhaeticus	—	—	x	†	—	—	x	†	not listed				—	—	x	†	not listed				—	—	x	†
Semiretisporis gothae	—	—	x	†	—	—	x	†	not listed				—	—	x, †	—	—	—	x	†	x	—	—	†
MR1 mass rarity	8	—	—	—	7	—	—	—	4	—	—	—	6	—	—	—	6	—	—	—	5	—	—	—
MR1 extinction	2	—	—	—	1	—	—	—	1	—	—	—	1	—	—	—	2	—	—	—	2	—	—	—
Crisis interval mass rarity	—	—	—	—	—	1	—	—	—	—	—	—	—	1	—	—	—	2	—	—	—	1	—	—
Crisis interval extinction	—	—	—	—	—	2	—	—	—	—	—	—	—	—	—	—	—	—	—	—	—	1	—	—
MR2 mass rarity	—	—	6	—	—	—	6	—	—	—	3	—	—	—	5	—	—	—	2	—	—	—	3	—
MR2 extinction	—	—	—	—	—	—	—	—	—	—	3	—	—	—	2	—	—	—	2	—	—	—	—	—
Post-crisis extinction	—	—	—	8	—	—	—	7	—	—	—	2	—	—	—	6	—	—	—	4	—	—	—	5

R = recovery.
x = rarity.
(x) = major decline.
†= extinction.

Limbosporites lundbladiae, Polypodiisporites polymicroforatus, Semiretisporis gothae and *Ricciisporites tuberculatus* exhibit mass rarity, while *Classopollis classoides, C. meyerianus* and *G. zwolinskai* again increase in abundance (**Table 3**; **Figure 5**). The recovery of *G. zwolinskai* is surprising, but this has also been documented in Mariental (see below). This contrasts to records further north where this taxon appears to have gone extinct during MR1 (Lund, 2003; Lindström et al., 2017a; this paper). *Semiretisporis gothae* and *R. germanicus* went extinct at this level. *Ovalipollis ovalis, Lunatisporites rhaeticus* and *Limbosporites lundbladiae* lingered on but disappeared during the post-crisis interval (**Table 2**; **Figure 5**). *Ricciisporites tuberculatus* increased again towards the top of the record (Gravendyck et al., 2020) similar to what is seen in Stenlille (**Figure 2**), and most likely went extinct at a higher level.

3.1.3 Mariental, Germany

In the Mariental succession (**Figure 1**), six taxa show marked abundance drops at a level equivalent to MR1 in the upper part of the Contorta Beds, namely *Classopollis* spp., *G. zwolinskai, Limbosporites lundbladiae, Ovalipollis ovalis, Perinopollenites elatoides* and *Rhaetipollis germanicus* (Heunisch et al., 2010). The latter as well as *Granuloperculatipollis rudis* went extinct at that level (**Figure 5**). A similar pattern was also noted by Lund (2003) in the German well Eitzendorff 8 located in the Bremen area, where a MFS in the upper part of the Mittel-Rhät Contorta Beds is marked by an acme of *R. rhaetica*, and succeeded by the last occurrences of *G. rudis*, *G. zwolinskai* and *R. germanicus* (Lund, 2003). During the middle part of the crisis interval (the Triletes beds) *Ricciisporites tuberculatus* and *Lunatisporites rhaeticus* exhibited mass rarity (Heunisch et al., 2010) (**Table 3**; **Figure 5**). The latter as well as *Limbosporites lundbladiae* disappeared at a level equivalent to MR2, where also *Polypodiisporites polymicroforatus* and *Semiretisporis gothae* show mass rarity. Four taxa, *O. ovalis, P. polymicroforatus, R. tuberculatus* and *Semiretisporis gothae* went extinct during the post-crisis interval (Heunisch et al., 2010) (**Table 2**; **Figure 5**). *Classopollis* spp., *Perinopollenites elatoides* and *Geopollis zwolinskai* all recovered during MR2 (Heunisch et al., 2010).

3.1.4 Kuhjoch, Austria

The Triassic–Jurassic boundary succession at Kuhjoch (**Figure 1** and) is the Global Stratigraphic Section and Point (GSSP) for the base of the Jurassic (Hillebrandt et al., 2013). Several of the herein compared taxa were not listed in the Kuhjoch record, including *G. zwolinskai, G. rudis, M. minimus* and *S. gothae* (**Table 3**; **Figure 5**), and two taxa, *P. elatoides* and *R. tuberculatus* were seemingly unaffected (Hillebrandt et al., 2013). The open marine Kössen Formation in succeeded by a sea-level fall and the deposition of the grey Tiefengraben Member of the Kendlback Formation (Hillebrandt et al., 2013). Major drops in abundances occur within an interval corresponding to MR1 affecting e.g. *C. meyerianus, C. classoides,* while *G. rudis* and *R. germanicus* exhibit mass rarity (Bonis et al., 2009) (**Table 3**; **Figure 5**). During the subsequent crisis interval, i.e. the Schattwald beds deposited during continued sea-level fall, mass rarity is registered in *L. lundbladiae, O. ovalis* and *L. rhaeticus*. There instead, *Polypodiisporites polymicroforatus* and other spores dominated the assemblages (Bonis et al., 2009). *Granuloperculatipollis rudis* and *R. germanicus* went extinct during MR1, while *Lunatisporites rhaeticus* was extirpated during the crisis interval (**Table 3**; **Figure 5**). At a narrow interval at the base of the Spelae CIE, *Polypodiisporites polymicroforatus, Limbosporites lundbladiae, Lunatisporites rhaeticus* and *Semiretisporis gothae* became rare and later disappeared during the earliest Jurassic (**Table 3**; **Figure 5**).

3.1.5 A Supraregional Pattern

The comparison with other high-resolution palynological records from the European epicontinental sea and the northern Tethys margin clearly shows that mass rarity in coastal and near-coastal lowland plants occurred in two phases on a supraregional scale. Although significant differences in the pollen records occur for some species, e.g. for *P. elatoides*, the taxodiacean/cupressacean parent plant of which is known to have survived the end-Triassic crisis. However, while it was severely suppressed during MR1 and in both the "grey siltstone" beds in the Stenlille wells and the Triletes beds of the German well Mariental (Heunisch et al., 2010), the parent plant of *P. elatoides* occurred consistently in low numbers and appeared unaffected at the other localities (**Table 3**). This is most likely related to the ecological and climatological preference of the taxodiacean/cupressacean parent plant, which was never abundant during the Rhaetian in the United Kingdom or Austria (Bonis et al., 2010) (Hillebrandt et al., 2013), as well as the depositional environment at each site.

3.2 The Onset of an Ecological Crisis

The magmatic activity in the Central Atlantic Magmatic Province may have affected the terrestrial ecosystem in multiple ways, following the flow chart in **Figure 6**. The successive abundance losses at MR1 were unprecedented during the Rhaetian of NW Europe. The preceding increase in richness, ID1, which signals intermediate levels of ecosystem stress, coincided with and immediately succeeded the Marshi CIE, believed to reflect added excess of light carbon to the carbon cycle as greenhouse gases (Hesselbo et al., 2002; Ruhl and Kürschner, 2011; Lindström et al., 2021), which may have included methane from magma-sediment interaction (Ruhl et al., 2011; Capriolo et al., 2021) (**Figure 4**). The local/regional effects of the subsequent global warming would likely have varied depending on the prevailing palaeoclimatic conditions at each site. The maximum values in species richness also coincided with increased Hg-loading and moderately increased occurrences of mutated fern spores (Lindström et al., 2019) interpreted to reflect volcanic emissions from CAMP volcanism (Thibodeau et al., 2016; Percival et al., 2017; Lindström et al., 2019; Lindström et al., 2021). Increased occurrences of mutated *Classopollis* pollen at a corresponding stratigraphical level in Germany (Gravendyck et al., 2020) further suggests that mutagenic stress also affected the cheirolepidiacean conifers. The mutagenesis could have been caused by Hg-toxicity as suggested for the ferns (Lindström et al., 2019), however, other heavy metal toxicities or increased UV-B

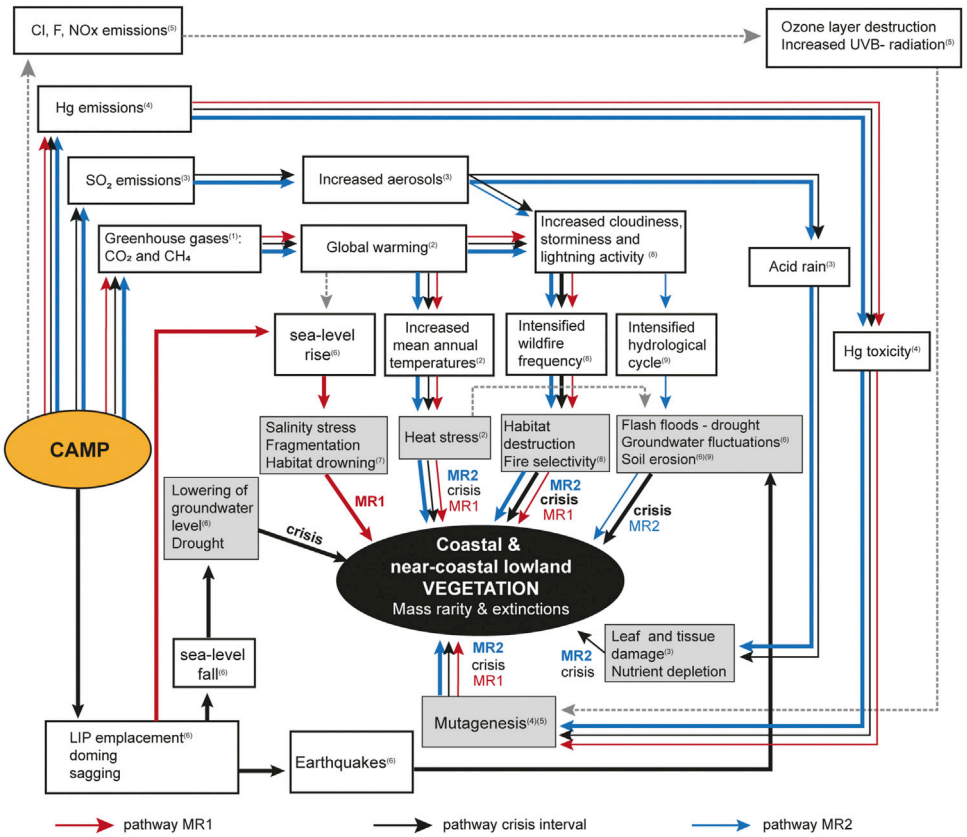

FIGURE 6 | Flow chart illustrating cause-and-effect relationships between the CAMP and the terrestrial vegetation. White boxes exemplify causes and primary physical effects of these, while secondary effects (physiological or directly affecting habitats) are marked with grey boxes. Different coloured arrows illustrate known or herein hypothesized pathways: red arrows = MR1; black arrows = crisis interval; and blue arrows = MR2. The thickness of the arrows emphasizes importance during the different intervals, with thicker lines being more important. Grey stippled arrows illustrate hypothesized pathways not discussed in detail in the text. Numbers in brackets refer to references that either hypothesise or have shown these possible pathways: 1) Hesselbo et al. (2002), Ruhl et al. (2011), Capriolo et al. (2021); 2) McElwain et al. (1999), Steinthorsdottir et al. (2011); 3) Guex et al. (2004), Lindström et al. (2012), Callegaro et al. (2014), Steinthorsdottir et al. (2018), Landwehrs et al. (2020); 4) Thibodeau et al. (2016), Percival et al. (2017), Lindström et al. (2019); 5) Heimdal et al. (2019), Benca et al. (2018); 6) Hallam and Wignall (1999), Hallam (1997), Nielsen (2003), Lindström et al. (2015), Weibel et al. (2016); 7) this paper; 8) Belcher et al. (2010), Petersen and Lindström (2012); 9) Steinthorsdottir et al. (2012), van de Schootbrugge et al. (2020).

radiation, as suggested for plant mutagenesis at the end-Permian event (Benca et al., 2018; Chu et al., 2021), cannot be excluded at this time (**Figure 6**).

3.3 The Effects of Rapid Sea-Level Changes

The coastal and near-coastal lowland terrestrial ecosystems along the margins of the European continental sea and the northern Tethys margin were vulnerable to sea-level changes, but the vegetation appears to have remained relatively stable during the middle Rhaetian. The black shale at the base of the Fjerritslev Formation was deposited during the late Rhaetian transgression (marked by a maximum flooding surface, MFS7; **Figure 2**) (Nielsen, 2003; Lindström and Erlström, 2006) which in contrast to previous transgressive events was associated with massive abundance losses in trees growing in coastal habitats or near-coastal lowlands during MR1 (**Figure 2**). The fact that this mass rarity occurred just prior to, during and after the culmination of this late Rhaetian transgression indicates that the rate of sea level rise outpaced the organic and inorganic sediment supply in the coastal region, leading to habitat fragmentation of the terrestrial coastal and lowland ecosystems to such an extent that it instigated the mass rarity (**Figure 6**). The fast relative sea-level rise in combination with global warming (Ruhl et al., 2011), increased wildfire frequency (Petersen and Lindström, 2012) and heavy metal pollution (Lindström et al., 2019) likely exerted profound stress on the terrestrial ecosystem at that time (**Figure 6**).

The late Rhaetian transgression was succeeded by a prominent regression during which the "grey siltstone beds" were deposited (**Figure 2**). This major drop in sea-level in the late Rhaetian was part of a regression-transgression couplet that can be recognized over large parts of Europe (Hallam, 1997; Hallam and Wignall, 1999), but the mechanism behind this sea-level drop remains to be explained. Hallam (1997) favoured a tectono-eustatic

mechanism other than sea-floor spreading, comparing it in pace and magnitude to glacio-eustacy. Hallam and Wignall (1999) suggested that the regression-transgression couplet was linked to the formation of the CAMP, and widespread occurrences of seismites in co-eval strata across Europe (Simms, 2003; Lindström et al., 2015) seem to support this. In the Danish Basin, this regression culminated with coastal deposition far into the basin, and in some marginal areas fluvial erosion and incision took place (Nielsen, 2003). As a consequence of this regression, a marked lowering of the base-level groundwater table would have had devastating effects on the remaining fragmented coastal mires and lowland ecosystems (**Figure 6**). Normally, sea-level changes affect the relative abundances of spores and pollen in such a way that wind-transported pollen increase in relative abundance compared to water-transported spores with increasing distance from the shore, i.e. the "Neves effect" (Chaloner and Muir, 1968). The fact that the opportunistic palynoflora dominated by *P. polymicroforatus, Deltoidospora* spp. and *Ricciisporites tuberculatus,* has been recovered from various terrestrial to marine settings (Lindström and Erlström, 2006; Lindström et al., 2017b) without major changes in the relative abundances, suggests that the floral shift was not due to the "Neves effect" (Chaloner and Muir, 1968), but that the deforestation on land was extensive (van de Schootbrugge et al., 2009).

On land, in northwest Scania in southern Sweden, the spore-pollen records indicate decreasing tree density from the middle to late Rhaetian, coincident with increased wildfire frequency but decreasing burning temperatures, where the latter may also reflect decreased tree density (Petersen and Lindström, 2012). In fluvial terrestrial strata, stratigraphically equivalent to the "grey siltstone" beds, perfectly zoned sphaerosiderite suggest strong seasonal climate variations with major fluctuations between high groundwater levels and drought (Weibel et al., 2016) (**Figure 6**). Fluctuations in groundwater levels could have been the result of extreme weather, with alternations between drought and excessive rain fall and flash floods during storms. It is also possible that changes in groundwater level was directly related to the on-going seismic activity (Weibel et al., 2016) (**Figure 6**). Both increased wildfire activity and deforestation would exacerbate sediment loads due to lack of vegetation stabilizing channel-margins and could potentially have hindered colonization of newly emerged surfaces by other than opportunistic plants. An abundance of reworked palynomorphs within the grey siltstone beds and equivalent strata in NW Europe, further suggest rapid ongoing soil erosion (van de Schootbrugge et al., 2020) (**Figure 6**).

Towards the top of this interval, increased species richness during ID2 (**Figure 4**) again indicate intermediate disturbance to the ecosystem. However, ID2 neither coincided with or immediately succeeded a negative $\delta^{13}C_{org}$ excursion or Hg-loading (Lindström et al., 2019) (**Figure 4**), hence disturbance stressing the opportunistic ecosystem at this level must have been something else. Multiple records provide evidence of further intensification of storminess and wildfire frequency at this level, as evidenced by charcoal records (Belcher et al., 2010; Petersen and Lindström, 2012), and pyrolytic polycyclic aromatic hydrocarbons (PAHs) (van de Schootbrugge et al., 2009; Lindström et al., 2021). In addition, PAH formed by incomplete combustion of organic matter suggest that intrusive coking of organic-rich sediments in the CAMP area also occurred (van de Schootbrugge et al., 2009). At the same level (Lindström et al., 2021), cuticles from bennettitaleans and ginkgoaleans in Greenland exhibit lesions and distortions typical of sulfuric acid deposition and this was further intensified across the TJB (Steinthorsdottir et al., 2018), suggesting ongoing sulphur-rich volcanic emissions from the CAMP, in line with that some CAMP lavas contained especially high levels sulphur compared to other LIPs (Callegaro et al., 2014). Acid rain would have exacerbated the physiological responses that TJB plants had to ongoing heat and water stress, possibly further increasing the hydrological cycle (Steinthorsdottir et al., 2012), which could explain why the opportunistic plants adapted to drought began to decline in abundance. MR2 preceded the prominent Spelae CIE (**Figures 2**, **4**). This negative excursion has been interpreted to reflect atmospheric increase in light carbon either through degassing of volcanic CO_2 or methane (Hesselbo et al., 2002; Ruhl et al., 2011). However, this was recently questioned by Fox et al. (2020) who instead suggested that the negative CIEs at the Spelae level were regional phenomena caused by fractionation by microbial mats under brackish water conditions. An increase in freshwater algae in the Stenlille record also seems to indicate enhanced runoff (Lindström et al., 2012), but because negative CIEs at the Spelae level are also present outside the European epicontinental sea, e.g. in Argentina (Ruhl et al., 2020), further studies are needed to resolve this issue. Regardless of which, the Spelae CIE did not instigate the MR2 mass rarity in land plants. Instead, living conditions for some of the plants that had suffered during MR1 (e.g. *Classopollis, Perinopollenites elatoides*) appear to have improved during the Spelae CIE, perhaps due to stabilizing climatic conditions. A second relative sea-level rise may have helped to restore some of the coastal and near-coastal lowland habitats that were lost during and after MR1 (**Figures 2–5**). Thus, at least in the northern hemisphere both the destruction and resurrection of coastal and near-coastal terrestrial ecosystems were tightly linked to relative sea-level changes.

3.4 Rare Species Are Especially Vulnerable to Climate and Environmental Change

Today, areas with long term stable climatic conditions have been found to contain higher numbers of rare plants, because of the reduced extinction risks (Enquist et al., 2019). However, because rare plants species are more susceptible to reductions in populations size, they are more likely to go extinct by orders of magnitude than more abundant species during times of rapid climate change (Enquist et al., 2019). The geographical and numerical reduction of plant species during the two end-Triassic mass rarity phases attest to the severe impact of this crisis on the vegetation in NW Europe.

The causality behind the mass rarity amongst the plants was clearly complex, including both direct effects of the volcanic activity in the CAMP, as well as subsequent feedback mechanisms. The volcanic activity of the CAMP emitted multiple stressors, including greenhouse gases, SO_2, Hg-pollution, PAHs, and likely also halocarbons (**Figure 6**). The results emphasize that rapid sea-level changes, probably driven by tectono-eustatic activity in the CAMP area, severely affected the coastal and near-coastal lowland vegetation, to the extent that many species already stressed by climate change and volcanic pollution, may have had difficulties coping with fragmentation of habitats and changes groundwater levels. The mass rarity was profound as it affected both already rare as well as previously abundant species and must have had a cascading negative impact on the terrestrial ecosystem as a whole, altering the conditions for a range of organisms from the lowest to the highest trophic levels. The mass rarity in plants was supraregional across NW Europe (**Table 2**), although small populations of typical Rhaetian plant taxa lingered without recovery into the earliest Jurassic (early Hettangian) in some areas. Most of these ghost taxa are only known by their spores or pollen and have not been identified as macroplant fossils, thus they were rare already prior to the crisis. Their extirpation in the aftermath of the end-Triassic crisis attest to the vulnerability of plant species to reductions in abundance and geographic range, especially in coastal regions. This should resonate when considering present day anthropogenic ecosystem disturbances and ongoing and future climate change scenarios (IPCC, 2021) that, similar to the end-Triassic crisis include rapid sea-level rise (De Conto et al., 2021) in combination with increased frequency and intensity of climate extremes such as prolonged heatwaves and drought, wildfires, major storms and heavy precipitation.

4 METHODS

4.1 Sampling, Palynological Processing and Analysis

109 sedimentary rock samples from Stenlille-1 and 87 ones from Stenlille-4 were processed using standard palynological methods at the Palynology Laboratory at GEUS. Approximately 20 g of each sample was crushed and treated with hydrochloric and hydrofluoric acids to remove carbonate and silicate minerals, respectively. Heavy minerals were removed from the residues using heavy liquid separation. The organic residues were mildly oxidized using nitric acid and filtered on 11 μm mesh filters. Strew slides were prepared after each step in the preparation after the hydrofluoric acid treatment, using glycerine gel as mounting medium. The palynomorph content of the samples were assessed by counting 300 specimens in one representative strew slide from each sample. Spore and pollen taxa abundances were normalized against the total spore-pollen count in each sample. It is important to remember that spore/pollen production in a plant is not necessarily related to the actual abundance of that plant in the ecosystem, and the parent plant of continuously rare spore/pollen taxa may still have played an important role in the ecosystem. In addition, plants that rely on insect or animal assistance with dispersal and pollination may have a more restrained pollen production compared to those that rely on wind for dispersal. In the late Triassic, prior to the diversification of the angiosperms, possible insect pollination has only been suggested for the Bennettitales (Labandeira et al., 2007).

Seventy-five samples from Stenlille-4 were analysed for palynofacies. Two-hundred particles or more were counted from each sample on the slide prepared after heavy liquid separation but prior to swirling. The palynodebris and palynomorphs were divided into ten different categories: *Black opaque phytoclasts* which include opaque usually rounded particles; *black wood* encompasses all black wood remains, both blade shaped, needle shaped and equidimensional ones; *plant tissue* includes all non-woody and non-cuticular plant remains; *cuticles* include translucent to semi-translucent tissue with cellular structures with or without stomata; *Amorphous organic matter (AOM)* encompasses degraded material either as structureless amorphous or structured amorphous matter; *marine phytoplankton* includes acritarchs, dinoflagellate cysts and prasinophytes, however, for graphic purposes unidentifiable palynomorphs were also included in this group but are listed separately in **Supplementary Table S3**; *freshwater microalgae* primarily include *Botryococcus braunii* and zygnematacean cysts; *Spores* also include rare fragments of clitellate cocoon fragments; and finally *pollen*. The counts are listed in **Supplementary Table S3**.

4.2 Mass Rarity Assessment

In palynology, loss of species abundance has often been used as an indicator of biotic crises without specifically referring this to mass rarity (Twitchett et al., 2001; Lindström and McLoughlin, 2007; van de Schootbrugge et al., 2009). The mass rarity of a taxon was determined as either: 1) a marked shift from consistently common to abundant abundance values to consistently or inconsistently rare occurrences, i.e. the last common occurrence (LCO), or 2) as a marked shift from consistently present in low abundances to inconsistently present in low or lower abundances, i.e. the last consistent occurrence (LCon). In fact, mass rarity is routinely used in palynostratigraphy as the last common occurrence (LCO) of a taxon, or for taxa of low abundance the last consistent occurrence (LCon) may also reflect mass rarity in the parent plant.

4.3 Diversity Patterns

Diversity trends in the successions were analyzed using species richness, dominance (1-Simpson index) and Pielou's evenness calculated using the software PAST4.05. Because many of the spore- and pollen-genera at the Triassic–Jurassic boundary are monospecific, species richness is only marginally higher than genus richness. Reworked taxa were excluded from the diversity analyses. The diversity patterns were assessed primarily according to the intermediate disturbance hypothesis (Connell, 1978; Svensson et al., 2012).

DATA AVAILABILITY STATEMENT

The original contributions presented in the study are included in the article/**Supplementary Material**, further inquiries can be directed to the corresponding author.

AUTHOR CONTRIBUTIONS

SL designed the project, produced and analysed the data, and wrote the manuscript.

FUNDING

This work was partly supported by the Geocenter Denmark grant 2013–6 to SL and the CCUS2020-project for providing support to the analyses of additional samples and compilation of data.

ACKNOWLEDGMENTS

SL would like to thank Gunver K. Pedersen and Lars Henrik Nielsen for comments on an early version of the manuscript. SL gratefully acknowledges the recent constructive reviews of Evelyn Kustatscher and Annette Götz.

SUPPLEMENTARY MATERIAL

The Supplementary Material for this article can be found online at: https://www.frontiersin.org/articles/10.3389/feart.2021.780343/full#supplementary-material

REFERENCES

Barbacka, M., Pacyna, G., Kocsis, Á. T., Jarzynka, A., Ziaja, J., and Bodor, E. (2017). Changes in Terrestrial Floras at the Triassic-Jurassic Boundary in Europe. *Palaeogeogr. Palaeoclimatol. Palaeoecol.* 480, 80–93. doi:10.1016/j.palaeo.2017.05.024

Belcher, C. M., Mander, L., Rein, G., Jervis, F. X., Haworth, M., Hesselbo, S. P., et al. (2010). Increased Fire Activity at the Triassic/Jurassic Boundary in Greenland Due to Climate-Driven floral Change. *Nat. Geosci* 3, 426–429. doi:10.1038/ngeo871

Benca, J. P., Duijnstee, I. A. P., and Looy, C. V. (2018). UV-B-induced forest Sterility: Implications of Ozone Shield Failure in Earth's Largest Extinction. *Sci. Adv.* 4, e1700618. doi:10.1126/sciadv.1700618

Bond, D. P. G., and Wignall, P. B. (2014). "Large Igneous Provinces and Mass Extinctions: An Update," in *Volcanism, Impacts, and Mass Extinctions: Causes and Effects* (Boulder, CO: G. Keller & A.C. Kerr.), 29–55. doi:10.1130/2014.2505(02)

Bonis, N. R., Kürschner, W. M., and Krystyn, L. (2009). A Detailed Palynological Study of the Triassic-Jurassic Transition in Key Sections of the Eiberg Basin (Northern Calcareous Alps, Austria). *Rev. Palaeobotany Palynology* 156, 376–400. doi:10.1016/j.revpalbo.2009.04.003

Bonis, N. R., Ruhl, M., and Kürschner, W. M. (2010). Milankovitch-scale Palynological Turnover across the Triassic-Jurassic Transition at St. Audrie's Bay, SW UK. *J. Geol. Soc.* 167, 877–888. doi:10.1144/0016-76492009-141

Callegaro, S., Baker, D. R., De Min, A., Marzoli, A., Geraki, K., Bertrand, H., et al. (2014). Microanalyses Link Sulfur from Large Igneous Provinces and Mesozoic Mass Extinctions. *Geology* 42, 895–898. doi:10.1130/g35983.1

Capriolo, M., Marzoli, A., Aradi, L. E., Ackerson, M. R., Bartoli, O., Callegaro, S., et al. (2021). Massive Methane Fluxing from Magma-Sediment Interaction in the End-Triassic Central Atlantic Magmatic Province. *Nat. Commun.* 12, 5534. doi:10.1038/s41467-021-25510-w

Chaloner, W. G., and Muir, M. (1968). "Spores and Floras," in *Coal and Coal-Bearing Strata*. Editors D. Murchison and T. S. Westall (Edinburgh: Oliver & Boyd), 127–146.

Chu, D., Dal Corso, J., Shu, W., Haijun, S., Wignall, P. B., Grasby, S. E., et al. (2021). Metal-induced Stress in Survivor Plants Following the End-Permian Collapse of Land Ecosystems. *Geology* 49, 657–661. doi:10.1130/g48333.1

Connell, J. H. (1978). Diversity in Tropical Rain Forests and Coral Reefs. *Science* 199, 1302–1310. doi:10.1126/science.199.4335.1302

De Conto, R. M., Pollard, D., Alley, R. B., Velicogna, I., Gasson, E., Gomez, N., et al. (2021). The Paris Climate Agreement and Future Sea-Level Rise from Antarctica. *Nature* 593, 83–89. doi:10.1038/s41586-021-03427-0

Enquist, B. J., Feng, X., Boyle, B., Maitner, B., Newman, E. A., Jørgensen, P. M., et al. (2019). The Commonness of Rarity: Global and Future Distribution of Rarity across Land Plants. *Sci. Adv.* 5, eaaz0414. doi:10.1126/sciadv.aaz0414

Fox, C. P., Cui, X., Whiteside, J. H., Olsen, P. E., Summons, R. E., and Grice, K. (2020). Molecular and Isotopic Evidence Reveals the End-Triassic Carbon Isotope Excursion Is Not from Massive Exogenous Light Carbon. *Proc. Natl. Acad. Sci. USA* 117, 30171–30178. doi:10.1073/pnas.1917661117

Gravendyck, J., Schobben, M., Bachelier, J. B., and Kürschner, W. M. (2020). Macroecological Patterns of the Terrestrial Vegetation History during the End-Triassic Biotic Crisis in the central European Basin: A Palynological Study of the Bonenburg Section (NW-Germany) and its Supra-regional Implications. *Glob. Planet. Change* 194, 103286. doi:10.1016/j.gloplacha.2020.103286

Guex, J., Bartolini, A., Atudorei, V., and Taylor, D. (2004). High-resolution Ammonite and Carbon Isotope Stratigraphy across the Triassic-Jurassic Boundary at New York Canyon (Nevada). *Earth Planet. Sci. Lett.* 225, 29–41. doi:10.1016/j.epsl.2004.06.006

Hallam, A. (1997). Estimates of the Amount and Rate of Sea-Level Change across the Rhaetian-Hettangian and Pliensbachian-Toarcian Boundaries (Latest Triassic to Early Jurassic). *J. Geol. Soc.* 154, 773–779. doi:10.1144/gsjgs.154.5.0773

Hallam, A., and Wignall, P. B. (1999). Mass Extinctions and Sea-Level Changes. *Earth-Science Rev.* 48, 217–250. doi:10.1016/s0012-8252(99)00055-0

Heimdal, T. H., Callegaro, S., Svensen, H. H., Jones, M. T., Pereira, E., and Planke, S. (2019). Evidence for Magma-Evaporite Interactions during the Emplacement of the Central Atlantic Magmatic Province (CAMP) in Brazil. *Earth Planet. Sci. Lett.* 506, 476–492. doi:10.1016/j.epsl.2018.11.018

Hesselbo, S. P., Robinson, S. A., Surlyk, F., and Piasecki, S. (2002). Terrestrial and marine Extinction at the Triassic-Jurassic Boundary Synchronized with Major Carbon-Cycle Perturbation: A Link to Initiation of Massive Volcanism? *Geol* 30, 251–254. doi:10.1130/0091-7613(2002)030<0251:tameat>2.0.co;2

Hesselbo, S. P., Robinson, S. A., and Surlyk, F. (2004). Sea-level Change and Facies Development across Potential Triassic-Jurassic Boundary Horizons, SW Britain. *J. Geol. Soc.* 161, 365–379. doi:10.1144/0016-764903-033

Heunisch, C., Luppold, F. W., Reinhardt, L., and Röhling, H.-G. (2010). Palynofazies, Bio- und Lithostratigrafie im Grenzbereich Trias/Jura in der Bohrung Mariental 1 (Lappwaldmulde, Ostniedersachsen). *zdgg* 161, 51–98. doi:10.1127/1860-1804/2010/0161-0051

Hillebrandt, A. v., Krystyn, L., Kürschner, W. M., Bonis, N. R., Ruhl, M., Richoz, S., et al. (2013). The Global Stratotype Sections and Point (GSSP) for the Base of the Jurassic System at Kuhjoch (Karwendel Mountains, Northern Calcareous Alps, Tyrol, Austria). *Episodes* 36, 162–198. doi:10.18814/epiiugs/2013/v36i3/001

Hull, P. M., Darroch, S. A. F., and Erwin, D. H. (2015). Rarity in Mass Extinctions and the Future of Ecosystems. *Nature* 528, 345–351. doi:10.1038/nature16160

Kürschner, W. M., Mander, L., and Mcelwain, J. C. (2014). A Gymnosperm Affinity for Ricciisporites Tuberculatus Lundblad: Implications for Vegetation and

Environmental Reconstructions in the Late Triassic. *Palaeobio Palaeoenv* 94, 295–305. doi:10.1007/s12549-014-0163-y

Labandeira, C. C., Kvaček, J., and Mostovski, M. B. (2007). Pollination Drops, Pollen, and Insect Pollination of Mesozoic Gymnosperms. *Taxon* 56, 663–695. doi:10.2307/25065852

Landwehrs, J. P., Feulner, G., Hofmann, M., and Petri, S. (2020). Climatic Fluctuations Modeled for Carbon and Sulfur Emissions from End-Triassic Volcanism. *Earth Planet. Sci. Lett.* 537, 116174. doi:10.1016/j.epsl.2020.116174

Lindström, S., Sanei, H., Van De Schootbrugge, B., Pedersen, G. K., Lesher, C. E., Tegner, C., et al. (2019). Volcanic Mercury and Mutagenesis in Land Plants during the End-Triassic Mass Extinction. *Sci. Adv.* 5, eaaw4018. doi:10.1126/sciadv.aaw4018

Lindström, S., Callegaro, S., Davies, J., Tegner, C., Van De Schootbrugge, B., Pedersen, G. K., et al. (2021). Tracing Volcanic Emissions from the Central Atlantic Magmatic Province in the Sedimentary Record. *Earth-Science Rev.* 212, 103444. doi:10.1016/j.earscirev.2020.103444

Lindström, S., Erlström, M., Piasecki, S., Nielsen, L. H., and Mathiesen, A. (2017a). Palynology and Terrestrial Ecosystem Change of the Middle Triassic to Lowermost Jurassic Succession of the Eastern Danish Basin. *Rev. Palaeobotany Palynology* 244, 65–95. doi:10.1016/j.revpalbo.2017.04.007

Lindström, S., and Erlström, M. (2006). The Late Rhaetian Transgression in Southern Sweden: Regional (And Global) Recognition and Relation to the Triassic-Jurassic Boundary. *Palaeogeogr. Palaeoclimatol. Palaeoecol.* 241, 339–372. doi:10.1016/j.palaeo.2006.04.006

Lindström, S., and McLoughlin, S. (2007). Synchronous Palynofloristic Extinction and Recovery after the End-Permian Event in the Prince Charles Mountains, Antarctica: Implications for Palynofloristic Turnover across Gondwana. *Rev. Palaeobotany Palynology* 145, 89–122. doi:10.1016/j.revpalbo.2006.09.002

Lindström, S. (2016). Palynofloral Patterns of Terrestrial Ecosystem Change during the End-Triassic Event - a Review. *Geol. Mag.* 153, 223–251. doi:10.1017/s0016756815000552

Lindström, S., Pedersen, G. K., Van De Schootbrugge, B., Hansen, K. H., Kuhlmann, N., Thein, J., et al. (2015). Intense and Widespread Seismicity during the End-Triassic Mass Extinction Due to Emplacement of a Large Igneous Province. *Geology* 43, 387–390. doi:10.1130/g36444.1

Lindström, S., Van De Schootbrugge, B., Dybkjaer, K., Pedersen, G. K., Fiebig, J., Nielsen, L. H., et al. (2012). No Causal Link between Terrestrial Ecosystem Change and Methane Release during the End-Triassic Mass Extinction. *Geology* 40, 531–534. doi:10.1130/g32928.1

Lindström, S., Van De Schootbrugge, B., Hansen, K. H., Pedersen, G. K., Alsen, P., Thibault, N., et al. (2017b). A New Correlation of Triassic-Jurassic Boundary Successions in NW Europe, Nevada and Peru, and the Central Atlantic Magmatic Province: A Time-Line for the End-Triassic Mass Extinction. *Palaeogeogr. Palaeoclimatol. Palaeoecol.* 478, 80–102. doi:10.1016/j.palaeo.2016.12.025

Lund, J. J. (2003). Rhaetian to Pliensbachian Palynostratigraphy of the central Part of the NW German Basin Exemplified by the Eitzendorf 8 Well. *CFS Courier Forschungsinstitut Senckenberg* 2003, 69–83.

McElwain, J. C., Beerling, D. J., and Woodward, F. I. (1999). Fossil Plants and Global Warming at the Triassic-Jurassic Boundary. *Science* 285, 1386–1390. doi:10.1126/science.285.5432.1386

McElwain, J. C., Popa, M. E., Hesselbo, S. P., Haworth, M., and Surlyk, F. (2007). Macroecological Responses of Terrestrial Vegetation to Climatic and Atmospheric Change across the Triassic/Jurassic Boundary in East Greenland. *Paleobiology* 33, 547–573. doi:10.1666/06026.1

McElwain, J. C., and Punyasena, S. W. (2007). Mass Extinction Events and the Plant Fossil Record. *Trends Ecol. Evol.* 22, 548–557. doi:10.1016/j.tree.2007.09.003

McGhee, G. R., Clapham, M. E., Sheehan, P. M., Bottjer, D. J., and Droser, M. L. (2013). A New Ecological-Severity Ranking of Major Phanerozoic Biodiversity Crises. *Palaeogeogr. Palaeoclimatol. Palaeoecol.* 370, 260–270. doi:10.1016/j.palaeo.2012.12.019

Mussard, J. M., Ducazeaux, J., and Cugny, P. (1997). Statistical Analyses of Palynomorph Assemblages in Middle Jurassic Deposits (Lower to Middle Bathonian, Brent Group, Norway). *Bull. Des Centres De Recherches Exploration-Production Elf Aquitaine* 21, 265–277.

Nielsen, L. H. (2003). Late Triassic - Jurassic Development of the Danish Basin and the Fennoscandian Border Zone, Southern Scandinavia. *GEUS Bull.* 1, 459–526. doi:10.34194/geusb.v1.4681

Percival, L. M. E., Ruhl, M., Hesselbo, S. P., Jenkyns, H. C., Mather, T. A., and Whiteside, J. H. (2017). Mercury Evidence for Pulsed Volcanism during the End-Triassic Mass Extinction. *Proc. Natl. Acad. Sci. USA* 114, 7929–7934. doi:10.1073/pnas.1705378114

Petersen, H. I., and Lindström, S. (2012). Synchronous Wildfire Activity Rise and Mire Deforestation at the Triassic-Jurassic Boundary. *Plos One* 7, e47236. doi:10.1371/journal.pone.0047236

Pott, C. (2014). A Revision of Wielandiella Angustifolia, a Shrub-Sized Bennettite from the Rhaetian-Hettangian of Scania, Sweden, and Jameson Land, Greenland. *Int. J. Plant Sci.* 175, 467–499. doi:10.1086/675577

Pott, C., and McLoughlin, S. (2011). The Rhaetian flora of Rögla, Northern Scania, Sweden. *Palaeontology* 54, 1025–1051. doi:10.1111/j.1475-4983.2011.01090.x

Pott, C., Schmeissner, S., Dütsch, G., and Van Konijnenburg-Van Cittert, J. H. A. (2016). Bennettitales in the Rhaetian flora of Wüstenwelsberg, Bavaria, Germany. *Rev. Palaeobotany Palynology* 232, 98–118. doi:10.1016/j.revpalbo.2016.04.010

Ruhl, M., Bonis, N. R., Reichart, G.-J., Damsté, J. S. S., and Kürschner, W. M. (2011). Atmospheric Carbon Injection Linked to End-Triassic Mass Extinction. *Science* 333, 430–434. doi:10.1126/science.1204255

Ruhl, M., Hesselbo, S. P., Al-Suwaidi, A., Jenkyns, H. C., Damborenea, S. E., Manceñido, M. O., et al. (2020). On the Onset of Central Atlantic Magmatic Province (CAMP) Volcanism and Environmental and Carbon-Cycle Change at the Triassic-Jurassic Transition (Neuquén Basin, Argentina). *Earth-Science Rev.* 208, 103229. doi:10.1016/j.earscirev.2020.103229

Ruhl, M., and Kürschner, W. M. (2011). Multiple Phases of Carbon Cycle Disturbance from Large Igneous Province Formation at the Triassic-Jurassic Transition. *Geology* 39, 431–434. doi:10.1130/g31680.1

Scheuring, B. W. (1970). Palynologische und palynostratigraphische Untersuchungen des Keupers im Bölchentunnel (Solothurner Jura). *Schweizerische Paläontologische Abhandlungen* 88, 119pp.

Sepkoski, J. J. (1996). "Patterns of Phanerozoic Extinction: a Perspective from Global Data Bases," in *Global Events and Event Stratigraphy*. Editor O. H. Walliser (Berlin: Springer-Verlag), 35–51. doi:10.1007/978-3-642-79634-0_4

Simms, M. J. (2003). Uniquely Extensive Seismite from the Latest Triassic of the United Kingdom: Evidence for Bolide Impact? *Geol* 31, 557–560. doi:10.1130/0091-7613(2003)031<0557:uesftl>2.0.co;2

Steinthorsdottir, M., Elliott-Kingston, C., and Bacon, K. L. (2018). Cuticle Surfaces of Fossil Plants as a Potential Proxy for Volcanic SO2 Emissions: Observations from the Triassic-Jurassic Transition of East Greenland. *Palaeobio Palaeoenv* 98, 49–69. doi:10.1007/s12549-017-0297-9

Steinthorsdottir, M., Jeram, A. J., and Mcelwain, J. C. (2011). Extremely Elevated CO2 Concentrations at the Triassic/Jurassic Boundary. *Palaeogeogr. Palaeoclimatol. Palaeoecol.* 308, 418–432. doi:10.1016/j.palaeo.2011.05.050

Steinthorsdottir, M., Woodward, F. I., Surlyk, F., and Mcelwain, J. C. (2012). Deep-time Evidence of a Link between Elevated CO2 Concentrations and Perturbations in the Hydrological Cycle via Drop in Plant Transpiration. *Geology* 40, 815–818. doi:10.1130/g33334.1

Stohlgren, T. J., and Kumar, S. (2013). "Endangered Plants," in *Encyclopedia of Biodiversity*. Editor S. A. Levin. Second ed (Academic Press Elsevier), 205–215. doi:10.1016/b978-0-12-384719-5.00241-0

Svensson, J. R., Lindegarth, M., Jonsson, P. R., and Pavia, H. (2012). Disturbance-diversity Models: what Do They Really Predict and How Are They Tested? *Proc. R. Soc. B.* 279, 2163–2170. doi:10.1098/rspb.2011.2620

Thibodeau, A. M., Ritterbush, K., Yager, J. A., West, A. J., Ibarra, Y., Bottjer, D. J., et al. (2016). Mercury Anomalies and the Timing of Biotic Recovery Following the End-Triassic Mass Extinction. *Nat. Commun.* 7, 11147. doi:10.1038/ncomms11147

Twitchett, R. J., Looy, C. V., Morante, R., Visscher, H., and Wignall, P. B. (2001). Rapid and Synchronous Collapse of marine and Terrestrial Ecosystems during the End-Permian Biotic Crisis. *Geol* 29, 351–354. doi:10.1130/0091-7613(2001)029<0351:rascom>2.0.co;2

van de Schootbrugge, B., Quan, T. M., Lindström, S., Püttmann, W., Heunisch, C., Pross, J., et al. (2009). Floral Changes across the Triassic/Jurassic Boundary Linked to Flood basalt Volcanism. *Nat. Geosci* 2, 589–594. doi:10.1038/ngeo577

van de Schootbrugge, B., Van Der Weijst, C. M. H., Hollaar, T. P., Vecoli, M., Strother, P. K., Kuhlmann, N., et al. (2020). Catastrophic Soil Loss Associated with End-Triassic Deforestation. *Earth-Science Rev.* 210, 103332. doi:10.1016/j.earscirev.2020.103332

Van Konijnenburg-Van Cittert, J. H. A., Pott, C., Schmeissner, S., Dütsch, G., and Kustatscher, E. (2020). Ferns and Fern Allies in the Rhaetian flora of Wüstenwelsberg, Bavaria, Germany. *Rev. Palaeobotany Palynology* 273, 104147. doi:10.1016/j.revpalbo.2019.104147

Van Konijnenburg-Van Cittert, J. H. A., Pott, C., Schmeissner, S., Dütsch, G., and Kustatscher, E. (2018). Seed Ferns and Cycads in the Rhaetian flora of Wüstenwelsberg, Bavaria, Germany. *Rev. Palaeobotany Palynology* 258, 190–214. doi:10.1016/j.revpalbo.2018.08.005

IPCC (2021). "Sixth Assessment Report," in *Climate Change 2021: The Physical Science Basis. Contribution of Working Group I to the Sixth Assessment Report of the Intergovernmental Panel on Climate Change*. Editors V. Masson-Delmotte, P. Zhai, A. Pirani, S. C. P. L. Connors, S. Berger, N. Caud, and et al (Cambridge: IPCC).

Weibel, R., Lindström, S., Pedersen, G. K., Johansson, L., Dybkjær, K., Whitehouse, M. J., et al. (2016). Groundwater Table Fluctuations Recorded in Zonation of Microbial Siderites from End-Triassic Strata. *Sediment. Geology.* 342, 47–65. doi:10.1016/j.sedgeo.2016.06.009

Conflict of Interest: The author declares that the research was conducted in the absence of any commercial or financial relationships that could be construed as a potential conflict of interest.

Publisher's Note: All claims expressed in this article are solely those of the authors and do not necessarily represent those of their affiliated organizations, or those of the publisher, the editors and the reviewers. Any product that may be evaluated in this article, or claim that may be made by its manufacturer, is not guaranteed or endorsed by the publisher.